Traffic 2008; **9:** 725–741
Blackwell Munksgaard

doi: 10.1111/j.1600-0854.2008.00722.x

Co-operative Versus Independent Transport of Different Cargoes by Kinesin-1

Jennetta W. Hammond[1], Kelly Griffin[1], Gloria T. Jih[1], Jeanne Stuckey[2] and Kristen J. Verhey[1,*]

[1]Department of Cell and Developmental Biology, University of Michigan, Ann Arbor, MI 48109, USA
[2]Department of Biological Chemistry, Life Sciences Institute, University of Michigan, Ann Arbor, MI 48109, USA
**Corresponding author: Kristen J. Verhey, kjverhey@umich.edu*

Kinesin motors drive the intracellular transport of multiple cargoes along microtubule tracks; yet, how kinesins discriminate among their many potential cargoes is unknown. We tested whether Kinesin-1 cargoes compete, co-operate or are transported independently of each other. We focused on Kinesin-1 cargoes that bind directly to the kinesin light chain (KLC) subunit, namely the c-Jun NH_2-terminal kinase-interacting proteins (JIPs) 1 and 3, Kidins220/ARMS and PAT1. Overexpression of individual cargo proteins in differentiated CAD cells resulted in mislocalization of the endogenous protein but had no effect on localization of other cargo proteins to neurite tips. Thus, while transport of distinct cargoes is saturable, they do not compete with each other. Interestingly, we found that low expression of JIP1 or JIP3 enhanced the transport of the other JIP to neurite tips. Moreover, JIP1 and JIP3 require each other for transport. Co-operative transport is due to an interaction between JIP1 and JIP3 as well as distinct binding sites on the KLC tetratricopeptide repeat (TPR) bundle: the TPR groove binds to C-terminal residues of JIP1, whereas the TPR surface binds to internal residues in JIP3. Formation of a JIP1/JIP3/KLC complex is necessary for efficient JIP1 or JIP3 transport in neuronal cells. Thus, JIP scaffolding proteins are transported in a co-operative manner, despite the independent transport of other Kinesin-1 cargoes.

Key words: cargo, JIP, JNK, kinesin, microtubule, TPR, transport

Received 6 August 2007, revised and accepted for publication 7 February 2008, uncorrected manuscript published online 11 February 2008, published online 10 March 2008

Motor proteins of the kinesin, myosin and dynein families utilize the energy of ATP hydrolysis to transport organelles, membrane vesicles and protein complexes along the cytoskeleton in order to organize cellular components for proper cell morphology and function (1,2). Critical to understanding the cellular roles of motor proteins is deciphering how motors attach to specific cargoes. Recent work has identified multiple binding partners for individual motor proteins. In some cases, these binding partners are soluble adaptor proteins that mediate the attachment of motor proteins to membrane-bound cargoes (2,3). How motor proteins distinguish cargo partners and bind to specific cargoes at specific times and cellular locations is unknown.

The founding member of the kinesin superfamily, Kinesin-1 (formerly conventional kinesin or Kif5), is a hetero-tetramer composed of two kinesin heavy chain (KHC) and two kinesin light chain (KLC) subunits. Both KHC and KLC have been implicated in cargo binding (4,5). For KLC, most cargoes bind to the tetratricopeptide repeat (TPR) bundle, although a role for the alternatively spliced C-terminal sequences has also been demonstrated (6,7). TPR bundles are protein–protein interaction domains composed of tandem TPR motifs. Each TPR motif contains a degenerate 34 amino acid repeat arranged in two antiparallel α-helices linked by a tight turn. Adjacent TPR motifs then pack against each other to form a half cylindrical bundle (8,9). Structural and biochemical analyses of the protein–protein interactions mediated by TPR domains have described two distinct mechanisms for partner protein binding. In several cases, the extreme C-terminal residues of the binding partner have been shown to bind in an extended conformation to the concave face (groove) of the TPR domain (10–12). Alternatively, internal sequences of the partner protein can bind to the loop regions that connect helices on the edge of the TPR bundle (13). Thus, target recognition by TPR domains is likely to be versatile and may enable the assembly of multiprotein complexes. Such an assembly function has been proposed for structurally similar helical repeat domains such as armadillo repeats, ankyrin repeats and 14-3-3 proteins (14–17).

The first cargo proteins identified to bind Kinesin-1 through the TPR bundle were the c-Jun NH_2-terminal kinase (JNK)-interacting protein (JIP) group of scaffold proteins (18–20). Based on their sequence similarities, JIPs can be divided into two classes (21). JIP1 [also called islet brain 1(IB1)] and JIP2 share a similar domain structure consisting of an N-terminal JNK-binding domain and C-terminal SH3 and PTB domains. JIP3 (also known as JSAP1) and JIP4 (also known as JLP) contain a JNK-binding domain and several coiled-coil domains. Despite this disparity in domain structure, the JIP proteins function as scaffolding proteins to co-ordinate the cellular localization and activity of JNK signaling complexes (21). Interestingly, the extreme C-terminal sequences of JIP1 and JIP2 are required for binding to the TPR bundle of KLC, whereas internal segments of JIP3

and JIP4 are required for KLC binding (18,20,22,23), suggesting that JIP1 binds in the TPR groove, whereas JIP3 binds outside of the TPR groove. Through their interactions with Kinesin-1, the JIPs likely also play a critical role in membrane trafficking as loss-of-function alleles of JIP homologues in *Caenorhabditis elegans* and *Drosophila* cause defects in axonal transport with phenotypes similar to KHC loss-of-function alleles (18,24,25).

In recent years, other cargoes that bind to Kinesin-1 through the TPR bundle have been identified, including Kidins220/ARMS, Calsyntenin/Alcadein, collapsin response mediator protein-2, Huntington-associated protein-1, Alzheimer precursor protein (APP), torsinA, 14-3-3 and Vaccinia virus's A36R protein (26–34). The identification of multiple cargoes for Kinesin-1 raises the question of how one motor coordinates the transport of its many potential cargoes. One possibility is that binding sites for different cargoes may not be accessible at the same time such that cargoes compete with each other for binding and transport (competitive transport model). A second possibility is that different cargoes may undergo co-operative transport whereby one cargo facilitates the binding and transport of another cargo (co-operative transport model). A third possibility is that different cargoes neither compete nor co-operate for transport but rather are transported independent of each other (independent transport model). We set out to test whether the transport of different cargoes by Kinesin-1 is competitive, co-operative or independent of each other. Our results suggest that transport of most Kinesin-1 cargoes that bind through the TPR bundle of KLC is not competitive but rather independent of each other. However, transport of JIP1 and JIP3 is co-operative because of interactions of JIP1 and JIP3 with KLC as well as with each other.

Results

Independent transport of the JIP proteins and other Kinesin-1 cargoes

As many different cargoes have been identified for Kinesin-1 (4,5), we focused on known binding partners of Kinesin-1 rather than organelles that can employ multiple motors through unknown linkage mechanisms. In addition, as both the KHC and KLC subunits have been implicated in Kinesin-1 cargo binding, we focused on cargo proteins that bind through the KLC subunit, specifically JIP1, JIP3, Kidins220/ARMS and PAT1. Kidins220/ARMS is a transmembrane protein whose cytoplasmic tail binds to KLC (27). Kinesin-1 activity is required for the transport of JIP1, JIP3 and Kidins220/ARMS to neurite tips in neuronal cells (19,20,27). PAT1 was identified as a binding partner of KLC in a yeast two-hybrid screen using the TPR motifs of KLC as the bait [(20) and data not shown], and the interaction between KLC and PAT1 has been confirmed by coimmunoprecipitation of glutathione S-transferase (GST)-tagged PAT1 and hemagglutinin (HA)-tagged KLC expressed in COS cells (Figure S1).

To test whether distinct cargoes are transported together or independent of each other, we first used live cell imaging of fluorescent protein (FP)-tagged cargoes. Unfortunately, we were unable to visualize JIPs undergoing transport in live cells, presumably because of the low number of molecules on a transport cargo [(24,35) and data not shown]. In addition, such studies cannot distinguish independent versus competitive transport. Thus, to test whether distinct Kinesin-1 cargo proteins are transported competitively, co-operatively or independent of each other, we used competition experiments in neuronal cells. We hypothesized that overexpression of one cargo should result in reduced transport and mislocalization of other cargoes if the two proteins compete for Kinesin-1-mediated transport, enhanced transport if the two proteins are transported co-operatively, and no effect on transport if the two proteins are transported independently.

We first explored the effect of overexpression of a cargo protein on the localization of its endogenous protein. Such experiments were feasible for JIP3 and Kidins220/ARMs using antibodies that recognize the endogenous proteins but not truncated KLC-binding constructs. Differentiated neuronal CAD cells were transfected with plasmids encoding the KLC-binding regions of JIP3 [Myc–JIP3 (138–621); Figure 5D] or Kidins220/ARMS [cyan fluorescent protein (CFP)–Kidins220/ARMS (1129–1426) (27) and Figure S1]. Overexpression of Myc–JIP3 (138–621) resulted in mislocalization of the endogenous JIP3 protein (Figure 1A,B) and overexpression of CFP–Kidins220/ARMS (1129–1426) interfered with transport of the endogenous Kidins220/ARMS protein (Figure 1C,D). These results indicate that competition for Kinesin-1 transport exists between transfected and endogenous cargo proteins. Thus, transport of individual Kinesin-1 cargoes is saturable.

We then tested the effect of overexpression of a cargo protein on the localization of other cargo proteins. Differentiated CAD cells were transfected with plasmids encoding green fluorescent protein (GFP)-tagged Kidins220/ARMS, and the localization of endogenous JIP1 and JIP3 was analyzed in transfected and untransfected cells. Overexpression of GFP–Kidins220/ARMS had no effect on the localization of JIP1 (Figure 2A,D) or JIP3 (Figure 2A,E) to neurite tips. As Kidins220/ARMS is a transmembrane protein and accumulates in the endoplasmic reticulum when overexpressed (Figure 1A and data not shown), we also tested whether overexpression of the KLC-binding region of Kidins220/ARMS as a soluble fragment could compete with JIP1 or JIP3 for Kinesin-1 transport. As with the full-length Kidins200/ARMS protein, overexpression of CFP–Kidins220/ARMS (1129–1426) had no effect on JIP1 (Figure 2A,D) or JIP3 (Figure 2A,E) localization. In the converse experiments, overexpression of Myc–JIP1 or Flag–JIP3 in differentiated CAD cells had no effect on the localization of endogenous Kidins220/ARMS protein to neurite tips (Figure 2B,F). These results indicate that Kidins220/ARMS and the JIPs do not compete for Kinesin-1 transport.

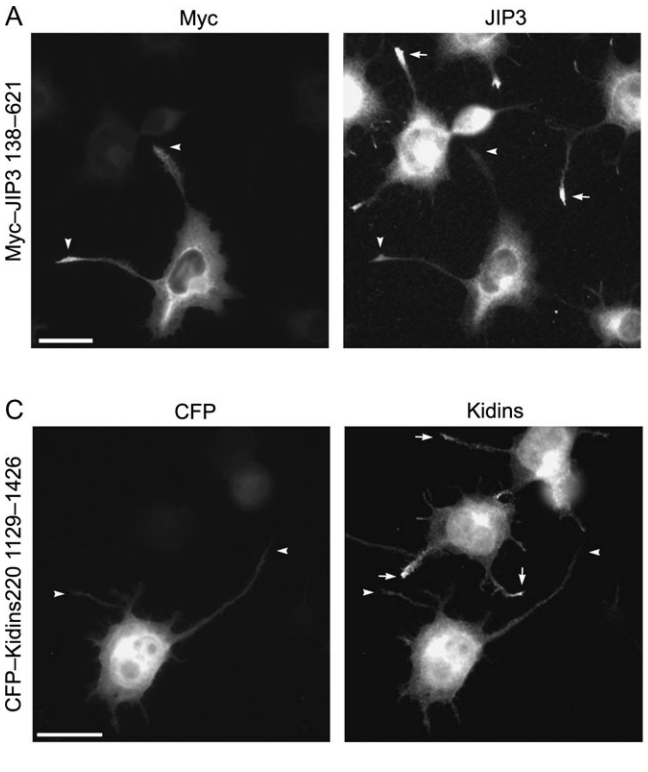

Figure 1: Transport of specific cargo proteins by Kinesin-1 is saturable. (A and C) Differentiated CAD cells overexpressing the KLC-binding region of (A) JIP3 [Myc–JIP3 (138–621)] or (C) Kidins220/ARMS [CFP–Kidins220/ARMS (1129–1426)] were fixed and stained for (A) the Myc tag and the endogenous JIP3 protein or (C) the Kidins220/ARMS protein. Arrowheads, neurite tips of transfected cells; arrows, neurite tips of non-transfected (NT) cells. Scale bar = 20 μm. (B and D) Quantification of endogenous (B) JIP3 or (D) Kidins220/ARMS fluorescence intensity at neurite tips of NT cells or cells overexpressing the indicated proteins. *$p < 0.01$. Error bars = ±SEM. $n > 100$ neurites for each construct.

Moreover, immunoprecipitation experiments indicate that there is no competition between Kidins220/ARMS and JIP1 or JIP3 for Kinesin-1 binding (Figure S2). Thus, the transport of distinct Kinesin-1 cargoes is saturable but not competitive with other cargoes.

Similar experiments were carried out to assess whether PAT1 and the JIPs could compete with each other for Kinesin-1 transport to neurite tips. Differentiated CAD cells were transfected with plasmids encoding Flag-tagged PAT1, and the localization of endogenous JIP1 and JIP3 was analyzed in transfected and untransfected cells. In cells overexpressing Flag–PAT1, the localization of endogenous JIP1 (Figure 2C,D) and JIP3 (Figure 2C,E) was similar to that of untransfected cells, suggesting that there is no competition between the PAT1 and the JIPs for Kinesin-1-mediated transport. Similar experiments to investigate the effect of JIP1 or JIP3 overexpression on PAT1 localization could not be performed because of a lack of suitable antibodies.

We further analyzed the ability of Kinesin-1 cargoes to be transported co-operatively, independently or competitively by analyzing whether cargoes that bind through the KHC subunit could compete with JIP1 or JIP3 for Kinesin-1-mediated transport in neuronal cells. Overexpression of p120catenin constructs that bind to KHC [full-length or an N-terminal truncation ΔN (36)] had no effect on the localization of JIP1 or JIP3 (Figure S3). These results indicate that there is no competition or co-operation for Kinesin-1-mediated transport but rather that transport of different Kinesin-1 cargoes is independent of each other.

JIP1 facilitates JIP3 transport by Kinesin-1 and vice versa

We next set out to determine whether different JIPs, namely JIP1 and JIP3, are transported by Kinesin-1 in a competitive, co-operative or independent manner. Differentiated CAD cells were transfected with plasmids encoding Myc-tagged full-length JIP1. In cells expressing high levels of Myc–JIP1, the amount of endogenous JIP3 localized at neurite tips was similar to that in untransfected cells (Figure 3A,C), suggesting that there is no competition between JIP1 and JIP3 for Kinesin-1-mediated transport. Surprisingly, in differentiated CAD cells expressing Myc–JIP1 at levels similar to the endogenous JIP1 protein (based on localization of the Myc-tagged protein to the neurite tip), there is a twofold increase in the amount of JIP3 at the tips of neurites (Figure 3B,C). Similar results were obtained (Figure 3C and data not shown) upon expression of a truncated version of JIP1 that binds both JIP3 and KLC but not JNK [Myc–JIP1 (307–711); Figure 6]. In contrast, low-level expression of Myc–JIP1 had no effect on the localization of endogenous Kidins220/ARMS and vice versa (Figure 2D,F). These results suggest that JIP1 facilitates transport of JIP3.

Similar experiments were carried out to test whether JIP3 could affect the transport of JIP1 by Kinesin-1. In differentiated CAD cells expressing high levels of full-length

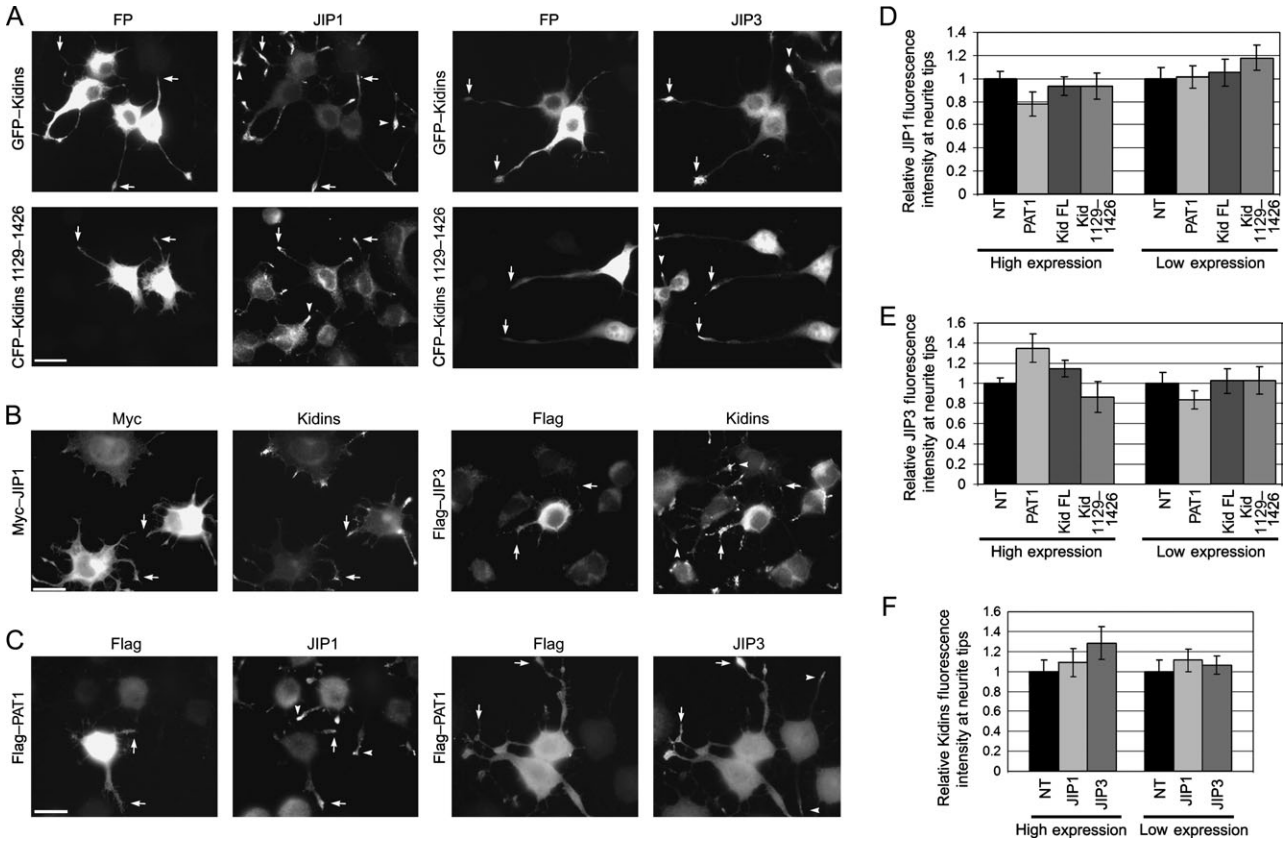

Figure 2: Kinesin-1 cargoes that bind through KLC do not compete with each other for transport. A) Differentiated CAD cells expressing GFP–Kidins220/ARMS or CFP–Kidins220/ARMS (1129–1426) were stained for the endogenous JIP1 (left set of panels) or JIP3 (right set of panels). B) Differentiated CAD cells expressing Myc–JIP1 (left panels) or Flag–JIP3 (right panels) were double labeled for the expressed proteins (Myc or Flag tags) and for the endogenous Kidins220/ARMS protein. C) Differentiated CAD cells expressing Flag–PAT1 were double labeled for the Flag tag and the endogenous JIP1 (left panels) or JIP3 (right panels). Arrows, neurite tips of transfected cells; arrowheads, neurite tips of non-transfected (NT) cells. Scale bar = 20 μm. (D–F) Quantification of (D) JIP1, (E) JIP3 and (F) Kidins220/ARMS fluorescence intensity at neurite tips of NT cells or cells overexpressing the indicated proteins. $n > 100$ neurites for each construct. Error bars = ±SEM. $p > 0.01$ for all transfected constructs.

Flag–JIP3 or a truncated version that binds both JIP1 and KLC [JIP3 (138–621); Figure 6], there was no change in the amount of endogenous JIP1 at neurite tips (Figure 3D,F). But in cells expressing low levels of Flag–JIP3 or JIP3 (138–621), there was an approximately 2- to 2.5-fold increase in the amount of JIP1 at neurite tips (Figure 3E,F). Low-level expression of Flag–JIP3 had no effect on the localization of endogenous Kidins220/ARMS and vice versa (Figure 2E,F). Thus, JIP3 facilitates transport of JIP1 by Kinesin-1.

JIP1 and JIP3 bind to different sites on the KLC TPR bundle

To undergo co-operative transport by Kinesin-1, JIP1 and JIP3 may co-operate for binding to the KLC subunit. To test this, Myc–JIP1, Flag–JIP3 and HA–KLC proteins were expressed separately in COS cells. Equal amounts of cell lysates were mixed together in various combinations prior to immunoprecipitating KLC with an anti-HA antibody. More Myc–JIP1 and Flag–JIP3 were coprecipitated with HA–KLC when all three proteins were present in the mixture than when the JIPs were present individually (Figure 4A,B). These results suggest that JIP1 and JIP3 co-operate for binding to the KLC TPR bundle and transport to neurite tips.

Previous studies on TPR-containing proteins identified two mechanisms of partner protein binding that may explain, at least in part, how JIP1 and JIP3 can co-operate for binding to the KLC TPR bundle. To identify sites in the KLC TPR bundle responsible for the interactions with JIP1 and JIP3, we undertook two approaches. In our first approach, we targeted specific residues for site-directed mutation based on a structural model of the KLC TPR repeats (Figure 4C). The sequences of TPRs 2–5 of rat KLC1-C (residues 247–411) were overlaid onto known crystal structures of other TPR bundles (Figure S4). Residues in the groove and along the edges of the KLC TPR bundle that are likely to be involved in partner protein binding (Figure 4C) were altered to alanine in the two-hybrid bait vector pGBD (20). In the BLUE mutant, charged residues in the loops that link

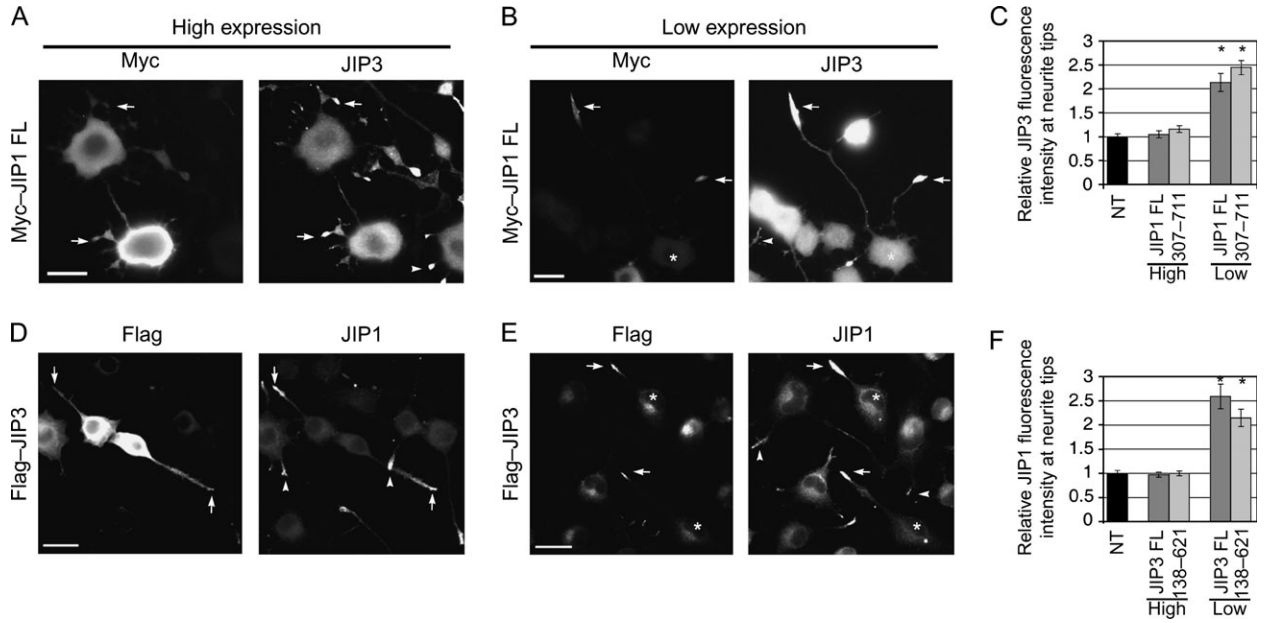

Figure 3: JIP1 facilitates JIP3s transport to neurite tips and JIP3 facilitates JIP1s transport. (A and B) Differentiated CAD cells expressing (A) high levels or (B) low levels of Myc-tagged JIP1 were fixed and stained with antibodies to the Myc tag and endogenous JIP3. Asterisk, cell body of transfected cell. Arrows, neurite tips of transfected cells; arrowheads, neurite tips of non-transfected (NT) cells. Scale bar = 20 μm. C) Quantification of JIP3 fluorescence intensity at neurite tips of NT cells or cells expressing high or low levels of full-length (JIP1 FL) or N-terminally truncated JIP1 (307–711). $n > 75$ neurites for each construct and expression level. Error bars = ±SEM. *$p < 0.01$. (D and E) Differentiated CAD cells expressing (D) high levels or (E) low levels of Flag-tagged JIP3 were fixed and stained with antibodies to the Flag tag and endogenous JIP1 protein. F) Quantification of JIP1 fluorescence intensity at neurite tips of NT cells or cells expressing high or low levels of full-length (JIP3 FL) or truncated JIP3 (138–621). $n > 150$ neurites for each construct and expression level. Error bars = ±SEM. *$p < 0.01$.

successive TPR repeats were altered, whereas in the ORANGE mutant, charged and/or bulky residues in the tight turns within a TPR repeat were altered (Figure 4C). The YELLOW and GREEN mutations targeted residues that (i) are conserved across many TPR bundles and (ii) whose side chains have been shown to project into the groove of other TPR bundles. Specifically, the YELLOW mutant targeted conserved asparagine residues that form a continuous ladder through the superhelix and play a critical role in binding the C-terminal peptide backbone of target proteins (10–12,37). The GREEN mutant targeted conserved hydrophobic residues in the TPR groove (Figure 4C). The ability of the mutant KLC TPR bundles to bind JIP1 and JIP3 was then tested in a directed two-hybrid assay. As shown in Figure 4D, mutations along the top of the TPR bundle (BLUE) abolished binding to both JIP1 and JIP3. Interestingly, mutations inside the TPR groove (YELLOW and GREEN) or along the bottom of the TRP bundle (ORANGE) abolished JIP1 binding but not JIP3 binding, suggesting that the C-terminal residues of JIP1 do indeed bind within the KLC TPR groove, whereas JIP3 binds through a different site.

In a second approach to identify residues in the KLC TPR bundle required for binding to JIP1 and JIP3, random mutagenesis of the KLC TPR bundle (amino acids 199–488) was carried out using error-prone polymerase chain reaction (EP-PCR). Most clones retained the ability to interact with both JIP1 and JIP3 in the directed two-hybrid assay. Sequencing revealed wild-type sequences (e.g. 14A; Figure 4D), single mutations (e.g. 27A; Figure 4D) or multiple mutations spread across the TPR bundle (e.g. 47A and 63A; Figure 4D). We identified several EP-PCR mutants that lost the ability to interact with JIP1 but retained an interaction with JIP3 (22A, 28A, 33A and 64A; Figure 4D). Sequencing of these clones showed that a variety of residues are involved in contacting the JIP1 C-terminal tail. Surprisingly, only one clone was identified that lost the ability to interact with JIP3 but retained an interaction with JIP1 (48A; Figure 4D). Consistent with previous results (23), two pieces of data suggest that the N-terminal half of the KLC TPR domain is critical for the KLC–JIP3 interaction. First, mutations that abolish JIP3 binding (clone 48A) are all clustered in the first three TPR motifs and second, a truncated TPR domain (clone 28A) that contains only the first 3.5 TPR motifs retains an interaction with JIP3. The fact that we have identified mutations that selectively abolish JIP1 or JIP3 binding suggests that the two scaffolding proteins bind to distinct sites and through distinct mechanisms to the TPR bundle. Specifically, these results support the hypothesis that the JIP1 C-terminal tail binds in the groove of the TPR bundle, whereas internal sequences in JIP3 bind outside the groove. This is the first demonstration that a single TPR domain can use distinct surfaces for binding different partner proteins.

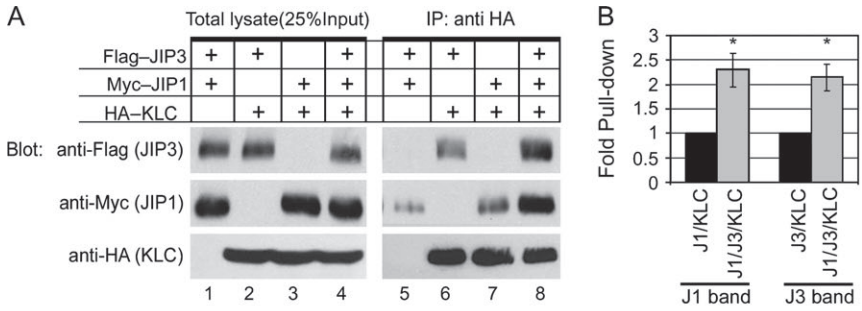

C

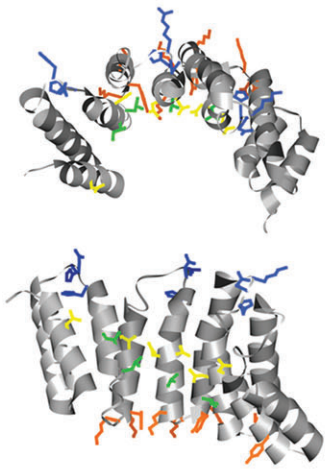

D

Yeast two-Hybrid			
KLC TPR mutant	Binds to JIP1?	Binds to JIP3?	Mutations
WT	yes	yes	Wild-type
BLUE	no	no	H249A, D250A, H251A, R291A, D292A, H293A, K333A, D334A, H335A
YELLOW	no	yes	N218A, N259A, N301A, N302A, N343A, N344A
GREEN	no	yes	I260A, L263A, V305A, L347A
ORANGE	no	yes	K270A, Y271A, K272A, K309A, K312A, Y313A, K314A, K354A, Y355A
EP-PCR #14A	yes	yes	Wild-type
EP-PCR #22A	no	yes	L300P, I326N
EP-PCR #27A	yes	yes	A202S
EP-PCR #28A	no	yes	R214C, L347stop
EP-PCR #33A	no	yes	N279A, C320Y, R327G, L347W, K382R, Y404F
EP-PCR #47A	yes	yes	A202V, G206S, A224V, R310C, V380M
EP-PCR #48A	yes	no	R214H, G227W, A232T, R310H, L319M, D334N
EP-PCR #63A	yes	yes	G205C, K312M, E435G, D459G
EP-PCR #64A	no	yes	E196G, A199T, N259S, L345Q, Q370P, Y391F, R433G
EP-PCR #66A	yes	yes	K270E, K354M

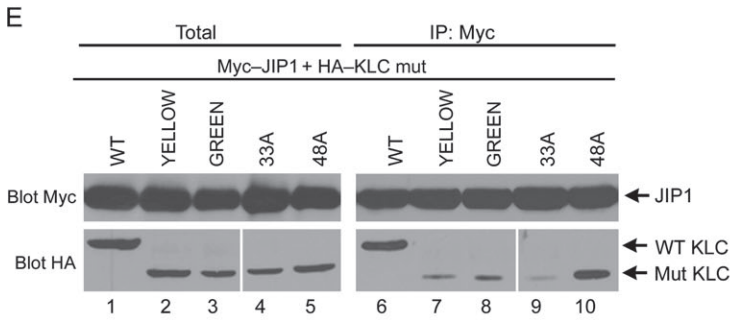

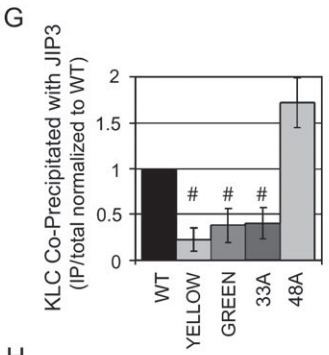

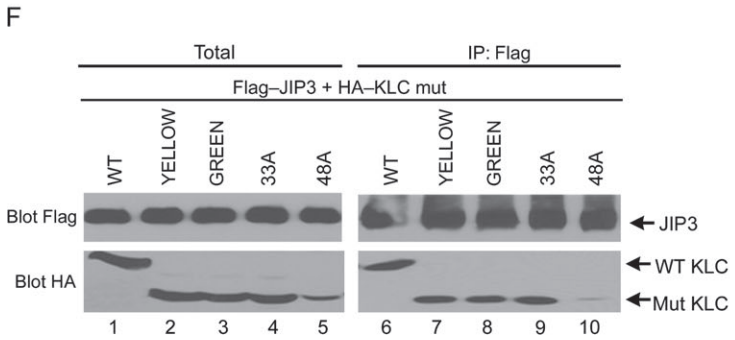

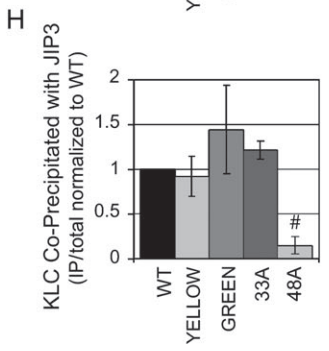

Figure 4: Legend on next page.

To confirm the binding specificity of these site-directed or EP-PCR mutants for JIP1 and JIP3 in mammalian cells, coimmunoprecipitation experiments were performed in COS cells as they contain minimal levels of endogenous Kinesin-1 and JIP proteins [(38,39) and data not shown]. For these experiments, truncated versions of the mutant KLC proteins were created as a result of ease of cloning because truncated (amino acids 1–488) and full-length (amino acids 1–560) versions of KLC display identical interactions with JIP1 and JIP3 [data not shown and (20)]. HA-tagged wild-type and mutant KLC proteins were coexpressed with either Myc–JIP1 or Flag–JIP3. Lysates were precipitated with antibodies to the Myc or Flag tags. Similar to the results of the directed two-hybrid assay, the YELLOW, GREEN and 33A mutants showed reduced binding to JIP1 (Figure 4E: lanes 7–9, Figure 4G) but not to JIP3 (Figure 4F: lanes 7–9, Figure 4H), whereas the 48A mutant showed reduced binding to JIP3 but not to JIP1 (Figure 4E,F: lane 10, Figure 4G,H). These results confirm that distinct residues in the KLC TPR bundle are responsible for the interactions with JIP1 and JIP3.

The two JIP binding sites on the KLC TPR bundle facilitate transport of the JIPs

To test whether both binding sites on the KLC TPR bundle contribute to the transport of JIP1 and JIP3, we expressed wild-type and mutant KLC TPR bundles in differentiated CAD cells. Overexpression of the wild-type KLC TPR bundle resulted in a loss of JIP1 and JIP3 tip localization by trapping cargo away from Kinesin-1 in a non-motile complex [Figure 5 and (20,40)]. We hypothesized that overexpression of a mutant KLC TPR bundle that retains an interaction with JIP3 but lost the interaction with JIP1 (e.g. GREEN; Figure 4) will have a dominant-negative effect on both JIP1 and JIP3 transport, and thus neurite tip localization, in the co-operative model but will selectively abolish only JIP3 transport if the JIPs can bind independently to KLC (independent model). As shown in Figure 5, overexpression of the GREEN mutant in differentiated CAD cells caused a significant decrease in both JIP1 (Figure 5A,C) and JIP3 (Figure 5B,D) tip localization. Similarly, overexpression of the 48A mutant that lost the interaction with JIP3 but retains an interaction with JIP1 (Figure 4) caused a significant decrease in both JIP1 (Figure 5A,C) and JIP3 (Figure 5B,D) tip localization. In control experiments, overexpression of the BLUE mutant, which lost the interaction with both JIP1 and JIP3 (Figure 4), had no effect on transport of either JIP protein (Figure 5). These results indicate that both JIP1 and JIP3 binding sites of the KLC TPR bundle contribute to JIP transport and support the conclusion that JIP1 and JIP3 are transported in a co-operative manner by Kinesin-1.

Oligomerization of JIP1 and JIP3

Binding of JIP1 and JIP3 to distinct sites on the KLC TPR bundle likely contributes to their co-operative transport. Yet, the possibility remained that JIP1 and JIP3 could interact with each other independent of their interaction with KLC. Binding as a JIP1/JIP3 oligomer could allow a stronger interaction with the two binding sites on KLC. Previous studies have shown that JIP1, JIP2 and JIP3 homo-oligomerize and that JIP2 can hetero-oligomerize with JIP1 and JIP3 (39,41,42). To test whether JIP1 can interact with JIP3, we performed coimmunoprecipitation experiments in transfected COS cells. When lysates expressing Myc–JIP1 and Flag–JIP3 were immunoprecipitated with an antibody to the Myc tag, both JIP1 and JIP3 were precipitated (Figure 6B: lane 9). Furthermore, the endogenous JIP1 and JIP3 in differentiated CAD cells hetero-oligomerize as shown by coimmunoprecipitation of JIP3 with an antibody to JIP1 (Figure 6F). Taken together, these results indicate that JIP1 and JIP3 can form an oligomeric complex. Thus, distinct binding sites on KLC for JIP1 and JIP3 and an interaction between JIP1 and JIP3 contribute to co-operative transport.

To define the regions of JIP1 responsible for the interactions with JIP3 and KLC, a series of Myc-tagged truncated and mutant versions of JIP1 were generated (Figure 6A). Full-length and truncated/mutant JIP1 proteins were coexpressed in COS cells with Flag–JIP3 (Figure 6B)

Figure 4: The KLC TPR domain contains distinct binding sites for JIP1 and JIP3, which facilitate co-operative binding. (A and B) Co-operative binding of JIP1 and JIP3 to KLC. Lysates of COS cells expressing Flag–JIP3, Myc–JIP1 or HA–KLC were combined and analyzed by Western blot either directly (total lysate) or after immunoprecipitation with an anti-HA antibody. B) Quantification from six independent experiments of the fold increase in JIP1 or JIP3 pull-down in the absence and presence of the other JIP. *$p < 0.01$; Error bars = ±SEM. C) Structural model of KLCs TPR motifs 1–5. The TPRs are depicted as a gray ribbon diagram. Residues targeted for mutation are depicted as ball-and-stick. The conserved asparagines across the concave face are indicated in YELLOW, whereas a series of hydrophobic residues that follow a similar line are shown in GREEN. The conserved K(Y/F)K residues within each TPR motif are shown in ORANGE, whereas the conserved basic residues in the loops that link successive TPR motifs are shown in BLUE. D) Results of directed yeast two-hybrid assay. Yeast expressing wild-type or the indicated mutant versions of the KLC TPR domain as bait were mated to yeast expressing JIP1 or JIP3 as prey. The residues targeted for mutation are indicated (BLUE, YELLOW, GREEN and ORANGE). For random mutation by EP-PCR, the mutated residues were determined after sequencing of the indicated clones. (E–H) Coimmunoprecipitation assay. COS cells were transiently transfected with plasmids encoding (E) Myc–JIP1 or (F) Flag–JIP3 along with wild-type (WT) or indicated mutant (Mut) KLC TPR proteins. Lysates were immunoprecipitated with (E) anti-Myc or (F) anti-Flag antibodies, separated by SDS–PAGE and immunoblotted with antibodies to the HA, Flag or Myc tags as indicated. (G and H) Western blot band intensities from three independent experiments were quantified using Image J. Shown is the percentage of total KLC (WT or Mut) that was co-immunoprecipitated with (E) JIP1 or (F) JIP3 normalized to WT. #$p < 0.05$; Error bars = ±SEM.

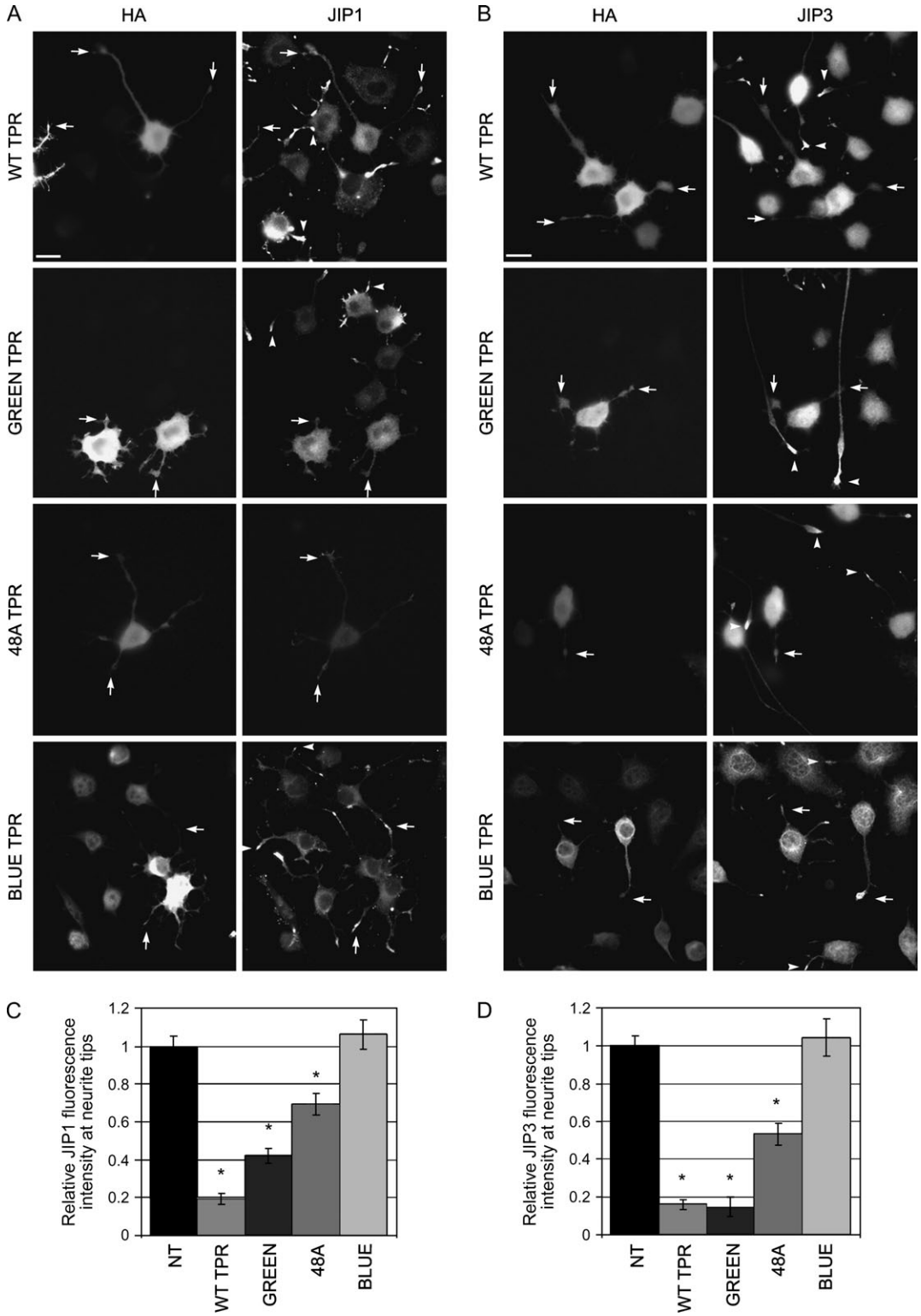

Figure 5: KLC TPR mutants functionally block both JIP1 and JIP3 transport to neurite tips. (A and B) Differentiated CAD cells expressing HA-tagged wild-type (WT) or mutant KLC TPR bundles (GREEN, 48A and BLUE) were double labeled for the HA tag and for endogenous (A) JIP1 or (B) JIP3. Arrows, neurite tips of transfected cells; arrowheads, neurite tips of non-transfected (NT) cells. Scale bar = 20 μm. (C and D) Quantification of (C) JIP1 or (D) JIP3 fluorescence intensity at neurite tips of NT cells or cells expressing the indicated WT or mutant TPR bundles. Compared with control NT cells, a significant (*$p < 0.01$) decrease in JIP1 or JIP3 staining intensity is seen in cells transfected with the WT, GREEN and 48A TPR bundles but not the BLUE TPR bundle. $n > 200$ neurites for each construct. Error bars = ±SEM.

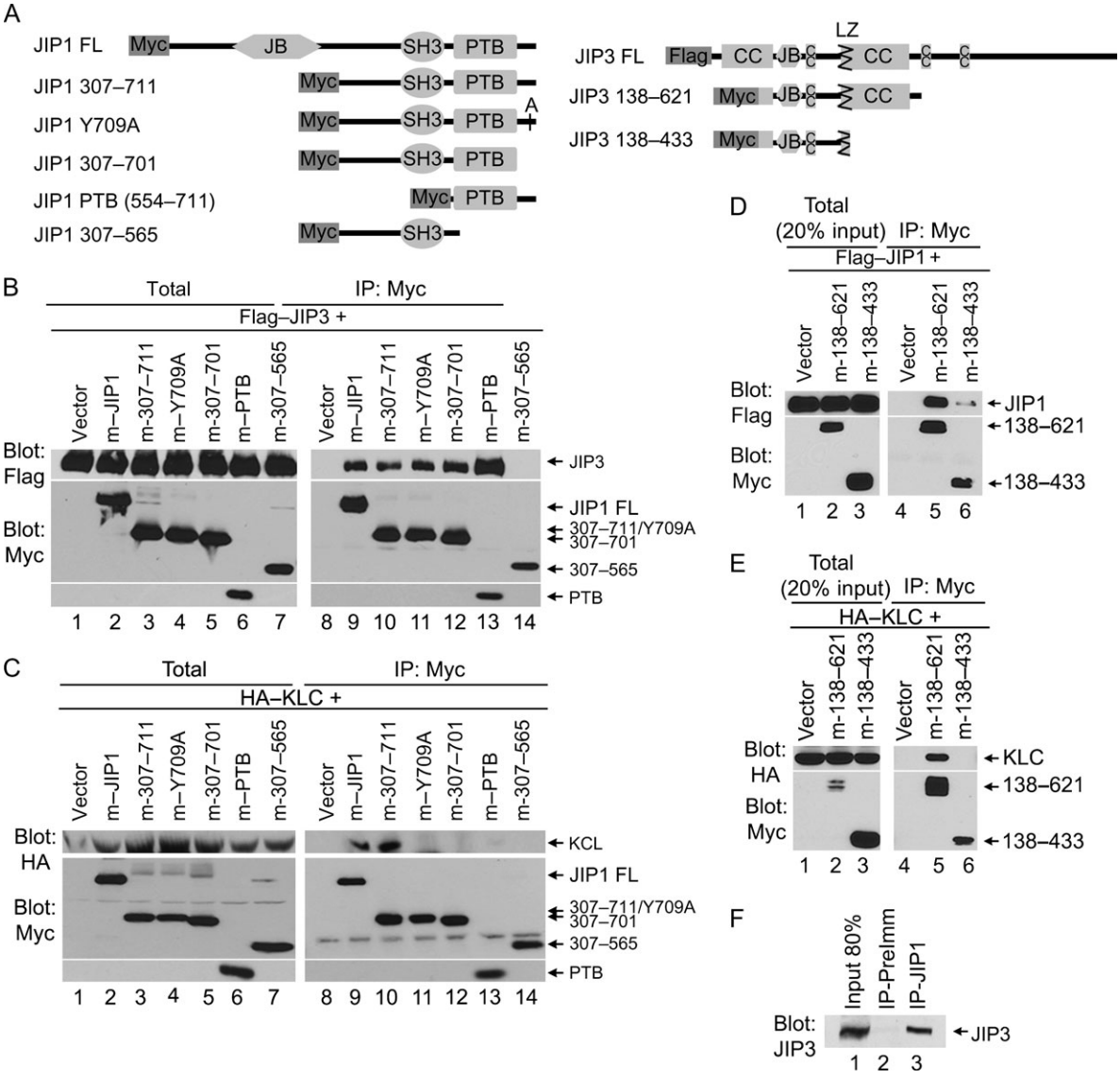

Figure 6: Oligomerization of JIP1 and JIP3. A) Schematic illustration of full-length (FL) or truncated JIP1 and JIP3 constructs. JB, JNK-binding domain; PTB, phosphotyrosine-binding domain; CC, coiled coil; LZ, leucine zipper. (B and C) Mapping of JIP1 domains. COS cells were cotransfected with the indicated Myc–JIP1 (m–JIP1) constructs and either (B) Flag–JIP3 or (C) HA–KLC. Cells were lysed and protein levels were analyzed by Western blot directly (total) or after immunoprecipitation (IP) with anti-Myc antibodies. (D and E) Mapping of JIP3 domains. COS cells were cotransfected with a control vector or the indicated Myc–JIP3 (m–JIP3) constructs and either (D) Flag–JIP1 or (E) HA–KLC. Cells were lysed and protein levels were analyzed by Western blot directly (total) or after immunoprecipitation (IP) with anti-Myc antibodies. F) Interaction between endogenous JIP1 and JIP3. Lysates of differentiated CAD cells were immunoprecipitated with an anti-JIP1 antibody (IP-JIP1) or with the control pre-immune serum (IP-PreImm). The presence JIP3 in the immunoprecipitate was determined by immunoblotting with an antibody to JIP3.

or HA–KLC (Figure 6C) and immunoprecipitated with an antibody to the Myc tag. JIP3 was coimmunoprecipitated with all of the truncated and mutated JIP1 proteins that contain an intact PTB domain (Figure 6B: lanes 9–13) but not with a construct containing just the SH3 domain of JIP1 (Figure 6B: lane 14). These results indicate that JIP3 interacts specifically with the PTB domain of JIP1. This binding region is distinct from the JIP1 sequences required for interaction with KLC as the coprecipitation of HA–KLC was lost upon mutation (Y709A; Figure 6C: lane 11) or truncation (307–701; Figure 6C: lane 12) of the C-terminal residues of JIP1, in agreement with previous results (20). Although the extreme C-terminal residues of JIP1 are necessary for the interaction with KLC, they are not sufficient as a construct containing only the PTB and C-terminal residues of JIP1 failed to coprecipitate KLC (Figure 6C: lane 13). These data indicate that JIP1 can form distinct interactions with JIP3 and KLC.

To define the regions of JIP3 required for the interactions with JIP1 and KLC, Myc-tagged truncated versions of JIP3 were created [(138–621) and (138–433); Figure 6A]. The truncated JIP3 proteins were coexpressed in COS cells with Flag–JIP1 (Figure 6D) or HA–KLC (Figure 6E) and immunoprecipitated with an antibody to the Myc tag. While the longer construct, JIP3 (138–621) coprecipitated both JIP1 (Figure 6D: lane 5) and KLC (Figure 6E: lane 5), the shorter fragment of JIP3 containing residues 138–433 interacted only weakly with JIP1 (Figure 6D: lane 6) and not at all with KLC (Figure 6E: lane 6). These results suggest that residues 138–433 of JIP3 are partly sufficient for the interaction with JIP1; however, residues 433–621 are required for complete JIP1 and KLC binding.

A JIP1/JIP3/KLC complex is necessary for efficient JIP1 or JIP3 binding and transport

Previously, we showed that KLCs binding sites for both JIP1 and JIP3 contribute to efficient transport of JIPs in neuronal cells (Figure 5). Having defined the regions of JIP1 and JIP3 required for binding KLC (Figure 6), we next tested whether JIP1 and JIP3 binding of the KLC TPR bundle is required for efficient transport of both JIPs. In control experiments, high-level expression of JIP1 constructs that bind both JIP3 and KLC [JIP1 (307–711); Figure 6] or that bind to neither JIP3 nor KLC [JIP1 (307–565); Figure 6] had no effect on localization of JIP3 to neurite tips (Figure 7A,B). Similar control experiments showed that high-level expression of JIP3 constructs that bind to both JIP1 and KLC [JIP3 full

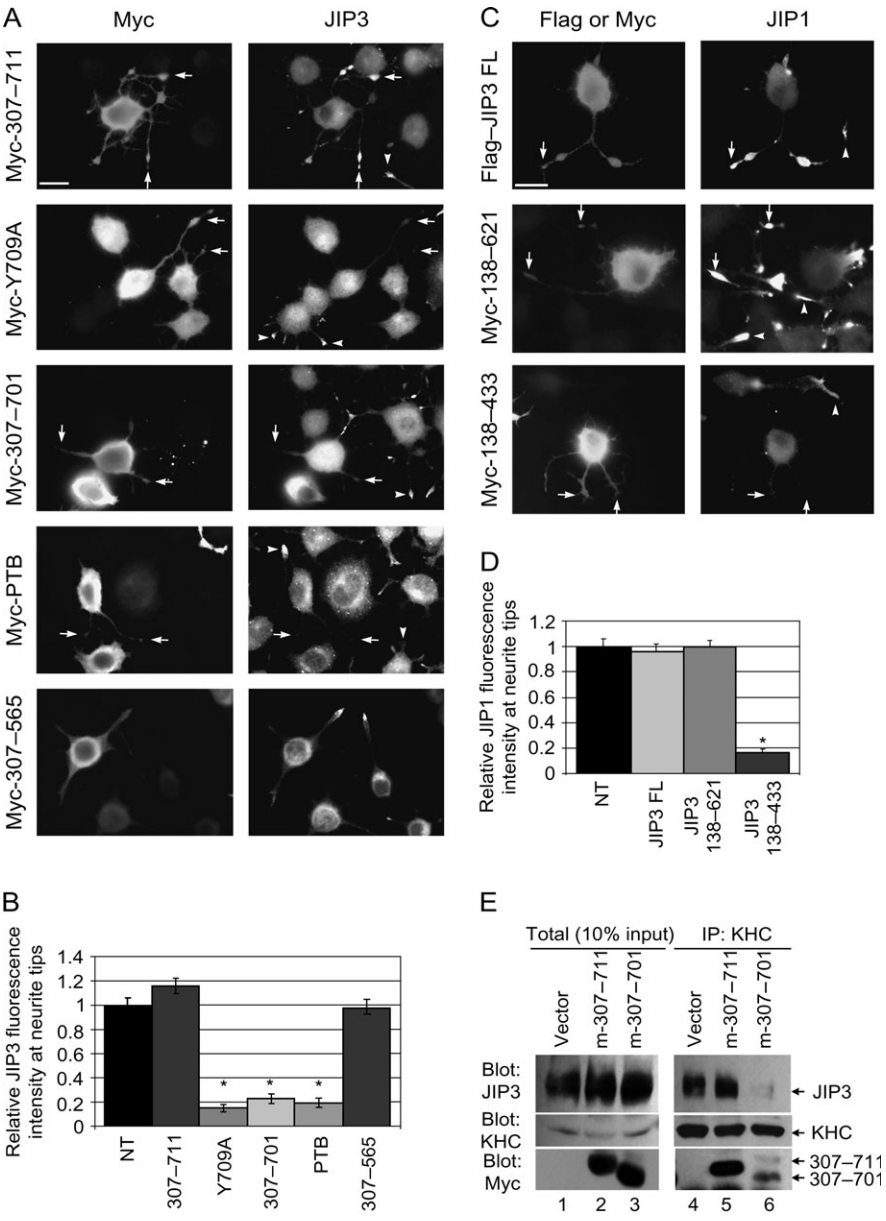

Figure 7: Interaction of JIP1 with KLC is required for JIP3 transport and vice versa. (A and B) Overexpression of JIP1 constructs. Differentiated CAD cells expressing the indicated truncated versions of Myc–JIP1 were immunostained with antibodies to the Myc tag and the endogenous JIP3 protein. Arrows, neurite tips of transfected cells; arrowheads, neurite tips of non-transfected (NT) cells. Scale bar = 20 μm. JIP3 fluorescence intensity at neurite tips was quantified (B) for NT cells or cells expressing the indicated JIP1 constructs. $n > 170$ neurites for each construct. Error bars = ±SEM. *$p < 0.01$. (C and D) Overexpression of JIP3 constructs. Differentiated CAD cells expressing full length (FL) Flag–JIP3 or the indicated truncated versions of Myc–JIP3 were immunostained with antibodies to the Flag or Myc tags and the endogenous JIP1 protein. JIP1 fluorescence intensity at neurite tips was quantified (D) for NT cells or cells expressing the indicated JIP3 constructs. $n > 200$ neurites for each construct. Error bars = ±SEM. *$p < 0.01$. E) Effect of JIP1 dominant negative constructs on JIP3 binding to KLC. Lysates of differentiated CAD cells expressing full-length or the indicated constructs of Myc–JIP1 were immunoprecipitated (IP) with antibodies to the endogenous KHC protein. Precipitates were analyzed by Western blot for the presence of the endogenous KHC and JIP3 proteins.

length and JIP3 (138–621); Figure 6] did not disrupt JIP1 transport (Figure 7C,D). In contrast, high expression of JIP1 proteins that bind JIP3 but not KLC [(307–701), Y709A and PTB; Figure 6] resulted in a significant decrease in the amount of JIP3 protein localized at neurite tips (Figure 7A,B). In addition, high expression of a JIP3 construct that binds weakly to JIP1 but not at all to KLC [JIP3 (138–433); Figure 6] resulted in a significant decrease in JIP1 levels at neurite tips (Figure 7C,D). These results suggest that although JIP1 and JIP3 can bind independently to the KLC TPR bundle, binding of both proteins to Kinesin-1 is required for efficient transport of the JIPs.

High expression of Myc–JIP1 (307–701) may act to disrupt JIP3 localization by preventing an efficient interaction of JIP3 with Kinesin-1. Upon overexpression of Myc–JIP1 (307–701) in differentiated CAD cells, less endogenous JIP3 protein was coimmunoprecipitated with Kinesin-1 (Figure 7E) compared with the vector control or expression of a JIP1 construct (307–711) that binds to both JIP3 and KLC (Figure 7E). These results suggest that high expression of Myc-JIP1 (307–701) results in a decreased interaction between endogenous JIP3 and Kinesin-1 proteins.

JIP1 is required for JIP3 transport and vice versa

To further explore the co-operative transport of JIP1 and JIP3 by Kinesin-1, we tested whether JIP1 is required for transport of JIP3 and vice versa using RNAi to knock down expression of JIP1 or JIP3 in differentiated CAD cells. To establish the knockdown efficiency and specificity of our shRNA plasmids, COS cells were cotransfected with mouse Flag–JIP1 or Flag–JIP3 and shRNA plasmids directed against JIP1 or JIP3. An empty shRNA vector was used as a control. Expression of the JIP1 shRNA plasmid resulted in decreased Flag–JIP1 expression (Figure 8A, lane 2), whereas Flag–JIP3 expression was unaffected (Figure 8B: lane 2). Expression of the JIP3 shRNA plasmid resulted in decreased JIP3 expression (Figure 8B: lane 3), whereas JIP1 expression was unaffected (Figure 8A: lane 3). Immunoblotting the same lysates for β-tubulin shows that equal protein levels were loaded.

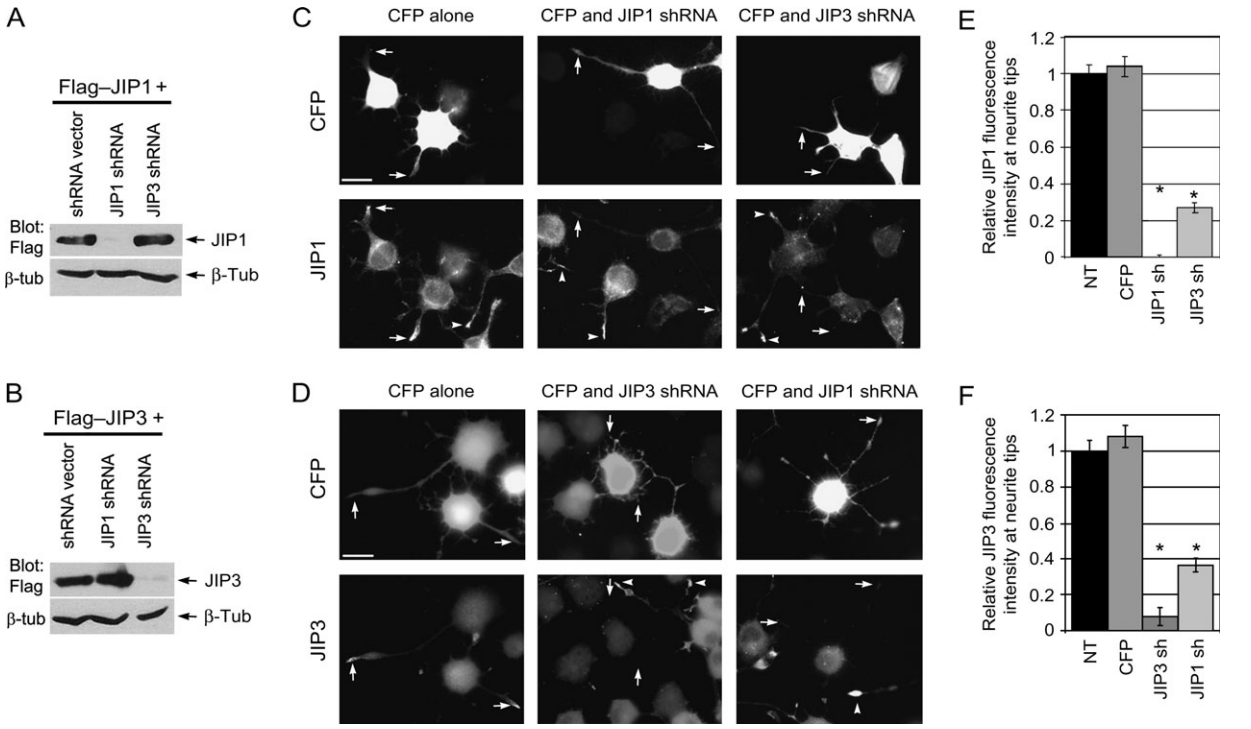

Figure 8: Knockdown of JIP1 abrogates JIP3 transport and vice versa. (A and B) Specificity of RNAi knockdown. COS cells were cotransfected with Flag–JIP1 (A) or Flag–JIP3 (B) and either an empty shRNA vector or shRNA plasmids targeting JIP1 or JIP3. The levels of remaining JIP1 and JIP3 were determined by immunoblotting total cell lysates with an anti-Flag antibody. Equal loading of total protein is indicated by blotting with an anti-β-tubulin antibody. (C and D) Differentiated CAD cells were transfected with a plasmid encoding CFP alone or together with JIP1 shRNA or JIP3 shRNA plasmids. Cells were fixed and immunostained with antibodies to the endogenous (C) JIP1 or (D) JIP3. Left panels: transfection with CFP has no effect on (C) JIP1 or (D) JIP3 tip localization or protein level. Middle panels: JIP1 and JIP3 shRNA-transfected cells show efficient knockdown of endogenous JIP1 or JIP3, respectively. Right panels: JIP3 shRNA-transfected cells show a defect in JIP1 tip localization (C) and JIP1 shRNA-transfected cells have a defect in JIP3 tip localization (D). Arrows, neurite tips of transfected cells; arrowheads, neurite tips of non-transfected (NT) cells. Scale bar = 20 μm. (E and F) Quantification of the relative JIP1 (E) or JIP3 (F) fluorescence intensity at neurite tips in transfected cells compared with NT cells. $n > 160$ neurites for each construct. Error bars = ±SEM. *$p < 0.01$.

The JIP1 or JIP3 shRNA plasmids were then transfected into differentiated CAD cells using a CFP plasmid as a marker for transfected cells. After 48 h, cells were fixed and immunostained for endogenous JIP1 or JIP3. Transfection of the shRNA plasmid against JIP1 resulted in loss of staining for endogenous JIP1 protein (Figure 8C,E), verifying the efficacy and specificity of the JIP1 shRNA construct, as well as a significant decrease in JIP3 localization at neurite tips (Figure 8D,F). Similarly, shRNA-mediated knockdown of JIP3 resulted in a loss of JIP3 staining (Figure 8D,F) as well as a significant decrease in JIP1 localization at neurite tips (Figure 8C,E). In the case of JIP3 knockdown, only cells that retained normal neurite morphology were selected for quantification as, in some cells, knockdown of JIP3 resulted in a complete loss of neurites or the formation of short, thin and highly branched neurites (data not shown) as previously observed (43,44). Taken together, the RNAi, dominant-negative and coimmunoprecipitation experiments support the conclusion that transport of JIP1 and JIP3 to neurite tips is dependent on the formation of a JIP1/JIP3/KLC complex.

Discussion

Co-operative versus independent transport of Kinesin-1 cargoes

To understand how motor proteins function in vesicle transport, it is important to determine how motors link to their cargoes and how transport is regulated. In the case of Kinesin-1, recent work has identified many proteins that bind to the KHC and KLC subunits (4,5). This raises several models for how transport of disparate cargoes by one motor might be co-ordinated. One possibility is that binding sites for different cargoes may not be accessible at the same time, such that cargoes compete with each other for transport. Our results suggest that this model is insufficient to describe cargo transport by Kinesin-1 as overexpression of cargoes that bind through KLC (Kidins220/ARMS, JIP1/JIP3 and PAT1) did not compete with other cargoes for transport. In addition, no competition was detected between cargoes that bind through KHC and those that bind through KLC (p120catenin and JIP1/JIP3, respectively). Overall, our results support a second model for co-ordination of multiple cargoes – that transport of disparate cargoes is saturable, yet independent of each other. The third model, co-operative transport, is viable in the case of Kinesin-1-mediated transport of JIP1 and JIP3 as these proteins bind to separate sites on the KLC TPR bundle, yet facilitate each other's binding and transport.

These results are compatible with those of Bracale et al. who showed that overexpression of the KLC-binding region of Kidins220/ARMS does not impair Kinesin-1 driven transport of Vaccinia virus to the plasma membrane (27). However, Araki et al. have shown that overexpression of JIP1 caused a reduction in anterograde velocity of GFP–Alcadein vesicles and reduced binding of Alcadein to KLC (26). Likewise, overexpression of Alcadein caused a reduction in anterograde velocity of APP–GFP vesicles (26). In addition, Horiuchi et al. have shown that overexpression of APLIP1, a JIP1 orthologue, in *Drosophila* causes defects in axonal transport (24). Further investigation, from the structural to the cellular level, is clearly required to understand how the transport of disparate cargoes is co-ordinated.

That transport of an individual cargo can be saturated yet not compete with other cargoes suggests that the Kinesin-1 motor is not rate limiting for transport. It has been suggested that the majority of Kinesin-1 protein, particularly in neuronal cells, is not participating in microtubule-based transport but rather is in a folded inactive state (4,38). This seemingly excess of Kinesin-1 protein may function to ensure an ample supply of motors that can be activated on demand. A similar mechanism may function in myosin-driven transport as mammalian myosin V is also regulated by autoinhibition (45,46).

The rate-limiting factor for Kinesin-1 transport may be unidentified accessory proteins required for selective cargo loading. In the case of JIPs, the formation of a JIP1/JIP3 oligomer may be rate limiting for Kinesin-1-mediated transport as low-level expression of either JIP1 or JIP3 enhanced transport of the other JIP protein. Yet, high-level expression of JIP1 or JIP3 may dilute out Kinesin-1/JIP cargo components and thus no longer enhance transport of the other JIP protein.

Our results are applicable to other cellular processes in which a diverse set of proteins depends on a common component for trafficking within the cell. Particularly relevant are studies showing that the clathrin-mediated endocytosis of disparate receptors and their ligands is saturable but not competitive (47). Recent work has shown that the rate-limiting factor is not the common clathrin core components but rather sorting connectors or adaptors that regulate the selective trafficking of specific cargoes (48). Whether kinesin-cargo interactions are regulated by similar mechanisms is unknown. In the case of cytoplasmic dynein, transport of a wide variety of cargoes is thought to derive from a diverse set of cargo-binding accessory polypeptides that bind to dynein heavy chain (49). These accessory polypeptides may bind in a mutually exclusive fashion to assemble distinct dynein-cargo combinations (50,51) or may bind simultaneously to assemble multi-cargo complexes (52). While overexpression of the light chain rp3 displaces the Tctex-1 light chain from dynein and blocks the apical delivery of rhodopsin (51), the differential tissue distribution of these light chains suggests that such competition may not exist *in vivo* (53).

Co-operative transport of JIP1 and JIP3 through a JIP1/JIP3/KLC complex

Our results show that although JIP1 and JIP3 can interact independently with KLC in yeast two-hybrid and coimmunoprecipitation experiments, they bind with higher

affinity when part of a complex (JIP1/JIP3/KLC). This complex is necessary for efficient JIP1 and JIP3 transport as evidenced by both RNAi knockdown and dominant negative expression experiments. Our demonstration of an interaction between JIP1 and JIP3 is in contrast to a previous report that JIP3 binds to the C-terminal PTB domain of JIP2 but not JIP1 (39). This discrepancy is most likely explained by the fact that the JIP1b splice variant (711 amino acids) used in this study contains a complete PTB domain, whereas the previous study likely used a shorter JIP1a splice variant (660 amino acids) containing only a partial PTB domain (42). Thus, a complete JIP1 PTB domain is required for the interaction of JIP1 with JIP3.

The biological significance of co-operative transport of JIP1 and JIP3 is not clear. Some reports have indicated that JIP1 and JIP3 play distinct roles in cellular processes such as stress signaling and apoptosis, cell migration and neuronal development (21,54). In our studies, we noticed that knockdown of JIP1 protein by RNAi resulted in increased neurite outgrowth, whereas loss of JIP3 protein resulted in decreased neurite outgrowth, similar to a previous report (44,55). However, recent reports have suggested that JIP1 and JIP3 can co-operate to control cellular events such as phosphorylation and accumulation of APP at neurite tips (44,55), axon guidance (56) and JNK activation following glucose deprivation (57). In this respect, co-operative transport of JIP1 and JIP3 by Kinesin-1 could facilitate the inclusion of many proteins into the transport complex and cross talk between unique subsets of JNK regulators and substrates (21,41,58). Indeed, the macromolecular complex transported by Kinesin-1 through JIP1 and JIP3 most likely includes multiple other proteins such as members of the JNK cascade and transmembrane receptor proteins (21,59).

Multiple mechanisms for partner protein binding by the KLC TPR domain

Our experiments indicate that the TPR bundle of KLC uses at least two independent regions for partner protein binding. First, the inside surface of the TPR groove binds to the extreme C-terminal residues of JIP1 similar to that of other TPR repeat-containing proteins such as Hop, PP5 and Pex5 and their interacting partners (10–12). Second, the outer convex surface of the TPR bundle binds to internal residues in JIP3 analogous to the binding interface of the TPR-containing protein $p67^{phox}$ and its partner Rac (13). Thus, although previous studies have demonstrated that both the groove and outer surfaces of TPR bundles can bind to partner proteins, KLC is the first TPR-containing protein known to utilize both mechanisms. In addition, in the case of KLC, these multiple interaction surfaces enable the co-operative assembly of a JIP1/JIP3/KLC complex.

Several features noted in other TPR bundles are important for JIP binding to KLC. First, substrate recognition and engagement by TPR bundles involves a variety of residues spread across a large surface area in the groove or along the outside of the TPR domain (8). Consistent with this, single mutations in the KLC TPR domain were not sufficient to abolish the interaction with JIP1 or JIP3. Second, an asparagine array lines the concave face of the bundle and likely contributes to peptide orientation in the groove (10–12,37). In the case of KLC, mutation of the asparagine array abolished the interaction with JIP1 but not with JIP3, supporting the conclusion that the C-terminal peptide of JIP1 sits in the KLC TPR groove.

KLCs TPR domain is known to mediate binding of Kinesin-1 to other proteins including Kidins220/ARMS, PAT1, Calsyntenin/Alcadein, collapsin response mediator protein-2, Huntington-associated protein-1, APP, torsinA, 14-3-3 and Vaccinia virus's A36R protein (26–34). In most of these cases, the mechanism of interaction is unknown as the residues required for binding have not been identified. In a recent study, quadruple mutations at positions L280, L287, A294 and L301 in KLC abolished the interaction with JLP, a JIP4 splice variant (23). Our structural model predicts that these residues contribute to helical packing between the second and third TPR motifs (data not shown). This is consistent with the structural function of residues in similar positions of the Leu-7 subclass of TPR-containing proteins (60). Thus, it seems likely that the loss of JLP binding was because of alterations in overall TPR domain structure rather than a novel leucine zipper interaction between KLC and JLP, as was proposed. Another recent study showed that two conserved WDDS motifs in the cytoplasmic C-terminal tail of Calsyntenin/Alcadein are required for efficient binding to KLC1 (26,33). As one WDDS is internal and the other within the last 10 amino acids, Calsyntenin/Alcadein may bind to KLC using either or both of the binding mechanisms identified in this study. Thus, it will be interesting to learn whether this diverse group of proteins binds to one of our two identified sites in KLCs TPR domain or whether the TPR bundle contains additional cargo-binding interfaces.

Materials and Methods

Plasmids

Plasmids encoding HA-tagged rat KLC1 and the six TPR motifs (amino acids 199–488) have been previously described (20,61). For coimmunoprecipitation with JIP1 and JIP3, mutant TPR domains from pGBD-KLC TPR were subcloned into pCDNA3-HA-KLC to create truncated mutant KLC proteins (amino acids 1–488) using convenient restrictions sites. For expression of wild-type and mutant KLC TPR domains as dominant negative proteins, mutant TPR domains were subcloned from pGBD-KLC TPR into pCDNA3-HA-KLC TPR (amino acids 199–488).

Flag-tagged mouse JIP1, JIP2 and JIP3 (39,42,62) were a kind gift of R. Davis (University of Massachusetts Medical School). The splice variant of JIP1 used in this study is JIP1b, also known as IB1, which contains the full PTB domain that the JIP1a variant lacks (42). Myc-tagged human full-length JIP1, as well as the truncations or mutants 307–711, Y709A, 307–701, and PTB (554–711) have been described previously (20,63). Myc-JIP1 (307–565) was generated by polymerase chain reaction (PCR) amplification using primers with convenient restrictions sites for cloning into the pRK5-Myc vector. Truncated JIP3 constructs [JIP3 (138–433) and (138–621)] were obtained

from clones identified in a yeast two-hybrid screen (20) and transferred from the two-hybrid prey vector pACT2 into the pCDNA3-myc vector. Flag–PAT1, GST–PAT1 (1–351) and GST–PAT1 (352–585) were a gift of J. Dictenberg and G. Bassell (Albert Einstein College of Medicine, Bronx, NY, USA). GFP–Kidins220/ARMS (27) was a gift from G. Schiavo (Cancer Research UK). CFP–Kidins220/ARMS (1129–1426) was subcloned from the full-length construct using convenient restriction sites. Enhanced cyan fluorescent protein (ECFP)–p120catenin and ECFP–p120cateninΔN2 (deletion of amino acids 28–233) (36) were a gift from K. J. Green (Northwestern University, Chicago, IL, USA).

Antibodies

The following antibodies were used: polyclonal and monoclonal antibodies to the Myc tag (Sigma C3956, Millipore 06-549 and 9E10 hybridoma ascites), HA tag (Sigma H6908, Upstate 07-221 and 12CA5 hybridoma ascites) and Flag tag (Sigma F7425 and Sigma F3165); polyclonal JIP1 [#152 (20)]; polyclonal JIP3 [against *Drosophila* JIP3 (Syd2) N-terminal residues 1–772 or C-terminal residues 1066–1328 (64), gifts from L. S. B. Goldstein, University of California, San Diego, CA, USA]; monoclonal and polyclonal Kidins220/ARMS [(27), gifts from G. Schiavo, Cancer Research UK]; monoclonal KHC (H2, Covance) and β-tubulin (E7, Developmental Studies Hybridoma Bank, University of Iowa, Iowa City, IA, USA). Polyclonal anti-KHC antibodies (B1-1) were generated against the KHC motor domain peptide CDKNRVPYVKGCTER (rat Kif5c amino acids 159–172). Secondary antibodies for immunofluorescence microscopy, fluorescein and rhodamine Red-X, were purchased from Jackson ImmunoResearch.

Structural model of KLC TPR motifs 1–5

The sequences of TPRs 2–5 of rat KLC1-C (residues 247–411) were overlaid onto crystal structures of other TPR bundles (Figure S4), specifically the TPR region of human Pex5 (PDB code 1FCH; residues A451–A552) and the TPR region of $p67^{phox}$ (PDB code 1E96; residues B120–B151) using the graphics program O (65). The first TPR of KLC (residues 210–246) was then modeled by spatial alignment with the helical regions of Pex5 (1FCH, residues A383–A445). The sixth TPR repeat of KLC could not be accurately represented in the model through sequence or structural alignments to other TPR regions because of a long insertion between the fifth and sixth TPR motifs that is unique to KLC.

Directed yeast two-hybrid assay

A construct containing the six TPR motifs (amino acids 199–488) of rat KLC1 in the two-hybrid bait vector pGBD has been described (20). Two-hybrid prey plasmids containing fragments of JIP1 and JIP3 in plasmid pACT2 were obtained in a two-hybrid screen (20). Directed mutation of specific residues in amino acids 199–370 of the KLC TPR domain was carried out by gene synthesis (66). EP-PCR to generate random mutations in KLC TPR motifs (amino acids 199–488) was carried out as described (67,68). Briefly, the region was amplified by PCR reactions in which MnCl was substituted for MgCl. Amplified products were subcloned back into the pGBD-KLC TPR plasmid using convenient restriction sites. Mutant clones were picked randomly and mini-prep DNA was transformed into the yeast strain AH109 (Clontech).

Screening of the mutant TPRs ability to bind to JIP1 and JIP3 was carried out by yeast mating. Yeast strain AH109 expressing wild-type or mutant pGBD-KLC TPR clones was mated to yeast strain Y189 expressing pACT2-JIP1 (478–711) or pACT2-JIP3 (138–680) in 96 well plates. Diploid yeast were sequentially plated on double (-leu,-trp) and triple (-leu,-trp,-his + 3-aminotriazole and -leu,-trp,-ade) drop-out plates. Successful mating was evidenced by growth on double drop-out (-leu,-trp) plates. A positive interaction between the KLC TPR domain and JIP1 or JIP3 was evidenced by growth on -leu,-trp,-his and on -leu,-trp,-ade drop-out plates.

Clones that lost the ability to interact with either JIP1 or JIP3 were selected for further analysis. Yeast plasmids were transformed back into *Escherichia coli* for DNA sequencing. A few clones that retained interactions with both JIP1 and JIP3 were also selected for DNA sequencing. In most cases, no mutations were found; however, in some cases, single or double mutations were found. Clones that lost the ability to interact with both JIP1 and JIP3 were not selected because these could include truncated KLC TPR domains as well as misfolded proteins.

Cell culture and fluorescence microscopy

COS and CAD cells were cultured as described (20) and transfected with *Trans*IT-LT1 (Mirus). Cells were processed for immunofluorescence as in Verhey et al. (20) and mounted in 50% glycerol, 0.5% *n*-propyl gallate in PBS or using Prolong Gold (Invitrogen). Images were collected with either an Olympus BX51 microscope with UplanFl 60X/NA 1.25 objective and Olympus DP70 CCD camera, or a Nikon TE2000 microscope Plan-Fl 40X/NA 0.75 or a Plan-APO 60X/NA 1.4 objective and Photometrics CS ES2 camera. Quantification of neurite tip immunofluorescence intensity was performed using Image J (National Institutes of Health). Neurite tips were hand-selected with an elliptical selection tool, and the average pixel fluorescence intensity was measured. In order to pool values from two or three independent experiments for statistical analysis (Student's *t*-test), measurements within each sample were normalized by first subtracting cell background fluorescence (determined from measurements within neurite shafts), then dividing each transfected or non-transfected tip measurement by the average intensity of all non-transfected neurite tips within the same experimental sample.

Immunoprecipitation

COS or CAD cells were resuspended in lysis buffer (40 mM HEPES, pH 7.5, 120 mM NaCl, 1 mM ethylenediaminetetraacetic acid, 10 mM sodium pyrophosphate, 10 mM β-glycerophosphate, 50 mM NaF, 0.5% NP40, 0.1% Brij-35 and protease inhibitors). Extracts were incubated with the specified antibodies for 2.5–18 h at 4°C then incubated with protein A agarose beads for 20 min at 4°C. Beads were washed two times with lysis buffer, resuspended in Laemmli sample buffer and analyzed by SDS–PAGE and Western blot.

RNAi

A shRNA (short hairpin RNA) plasmid targeting mouse JIP1 was made using DNA oligos designed with a 19mer sense sequence (selected using Dharmacon's website), 9 nucleotide loop, 19mer antisense sequence and 6T pol III stop sequence (sense: 5′-tttGGCTCACCGTGCACTTTAAttcaagagaTTAAAGTGCACGGTGAGCCtttttt-3′ and antisense: 5′-ctagaaaaaaGACCGTGTGTCTCGATCATtctcttgaaATGATCGAGACACACGGT-3′). Annealed oligos were cloned into the Bbs1 and Xba1 sites of the pU6-puro vector [modified from pU6pro (69) by addition of a puromycin resistance gene into the PvuII site]. The shRNA plasmid targeting mouse JIP3 was made the same way using a previously verified JIP3 shRNA sequence (70) (sense: 5′-tttGCAGGCCGAGGAGAAATTCAttcaagagaTGAATTTCTCCTCGGC CTGtttttt-3′ and antisense:5′-ctagaaaaaaCAGGCCGAGGAGAAATTCAtctcttgaaTGAATTTCTCCTCGGCCTG-3′). All plasmids were verified by DNA sequencing. Knockdown efficiency was verified by cotransfecting the shRNA or control plasmids into COS cells with Flag-tagged mouse JIP1 or JIP3 plasmids. Protein expression of Flag–JIP1 or JIP3 in control and knockdown cells was analyzed by Western blot and immunofluorescence.

Acknowledgments

We are grateful to L. Goldstein for antibodies to JIP3/Sunday Driver, G. Schiavo for antibodies and plasmids for Kidins220/ARMS, J. Dictenberg and G. Bassel for PAT1 plasmids and K. Green for p120catenin constructs. We thank B. Hammond, L. Weisman and members of the Verhey laboratory for valuable help and discussions. This work was supported in part by a grant from the National Institutes of Health to K. J. V (GM070862).

Supplementary Materials

Figure S1: Binding of Kidins220/ARMS and PAT1 to KLC. A) Schematic illustration of full-length Kidins220/ARMS and the truncated, cytoplasmic

construct CFP–Kidins220/ARMS (1129–1426). Ank, ankyrin repeats; TM, transmembrane domains; SD, SAM domain; KLC BD, KLC-binding domain as determined by (27) PDZ BM, PDZ binding motif. B) Coimmunoprecipitation of Kidins220/ARMS with KLC. Lysate from COS cells transfected with CFP–Kidins220/ARMS (1129–1426) was mixed with lysate from untransfected cells or cells transfected with HA–KLC. Mixed lysates were then immunoprecipitated with anti-HA antibodies and analyzed by Western blot. C) Schematic illustration of PAT1 and truncated GST–PAT1 constructs. D) GST–PAT1 (1–351) or GST–PAT1 (352–585) recombinant proteins were mixed with lysates from COS cells that had been transfected with HA–KLC or left untransfected. Mixtures were immunoprecipitated with anti-HA antibodies and analyzed by Western blot. KLC binds within amino acids 1–351 of PAT1.

Figure S2: Kidins220/ARMS does not compete with JIP1 or JIP3 for binding to KLC. Lysates of COS cells expressing Myc–JIP1, Flag–JIP3, CFP–Kidins220/ARMS (1129–1426) and HA–KLC were combined and analyzed by Western blot either directly (total lysate) or after immunoprecipitation with an anti-HA antibody. (A and B) Kidins220/ARMS and JIP1 do not compete for binding to KLC. A) Representative Western blot of coimmunoprecipitation of JIP1 and Kidins220/ARMS with KLC. Coprecipitation of Kidins220/ARMS with KLC (lane 6) or of JIP1 with KLC (lane 7) is not altered by the presence of the other cargo protein (lane 8). B) Quantification of five independent experiments. Error bars = ±SEM. $p > 0.05$ for all combinations. (C and D) Kidins220/ARMS and JIP3 do not compete for binding to KLC. C) Representative Western blot of coimmunoprecipitation of JIP3 and Kidins220/ARMS with KLC. Coprecipitation of Kidins220/ARMS with KLC (lane 6) or of JIP3 with KLC (lane 7) is not altered by the presence of the other cargo protein (lane 8). D) Quantification of six independent experiments. Error bars = ±SEM. $p > 0.05$ for all combinations.

Figure S3: p120catenin, a KHC-binding Kinesin-1 cargo, does not compete with JIP1 or JIP3 for transport. A) Differentiated CAD cells expressing CFP–p120catenin or an N-terminally truncated version of p120catenin, ΔN, were stained for endogenous JIP1 (left panels) or JIP3 (right panels). Arrows, neurite tips of transfected cells; arrowheads, neurite tips of non-transfected (NT) cells. Scale bar = 20 μm. (B and C) Quantification of JIP1 (B) or JIP3 (C) fluorescence intensity at neurite tips of NT cells or cells transfected with the indicated p120catenin construct. $n > 100$ neurites for each construct. Error bars = ±SEM. $p > 0.01$ for all transfected constructs.

Figure S4: Alignment of the structural model of KLC TPR repeats 1–5 with known TPR domain structures. The sequences of TPRs 2–5 of rat KLC1-C were overlaid onto the known crystal structures of human Pex5 and $p67^{phox}$. The first TPR of KLC (residues 210–246) was then modeled by spatial alignment with the helical regions of Pex5. The sixth TPR repeat of KLC could not accurately be represented in the model through sequence or structural alignments to other TPR regions because of a long insertion between the fifth and sixth TPR motifs that is unique to KLC. A) Ribbon diagrams depicting the structural alignment of the TPR domains of $p67^{phox}$ residues B2–B186 (red, PDB code 1E96) aligned with the model of KLC1, residues 210–411, shown in yellow. B) Manual alignment of the Ca atoms of the TPR region of the KLC1 structural model with four known TPR crystal structures. Yellow, KLC1 residues 210–411. Magenta, PP5 residues 19–170 (PDB code: 1A17). Blue, Hop residues A2–A118 (PDB code 1ELW). Red, $p67^{phox}$ residues B2–B186 (PDB code 1E96). Green, Pex5 residues A420–A602 (PDB code 1FCH). Depicted in brown are the cocrystalized binding partners of Hop [Hsp70 C-terminal peptide (C5–C12), PDB code 1ELW] and $p67^{phox}$ [peroxisomal targeting peptide (C1–C5), PDB code 1E96].

Supplemental materials are available as part of the online article at http://www.blackwell-synergy.com

References

1. Caviston JP, Holzbaur EL. Microtubule motors at the intersection of trafficking and transport. Trends Cell Biol 2006;16:530–537.
2. Hirokawa N, Takemura R. Molecular motors and mechanisms of directional transport in neurons. Nat Rev Neurosci 2005;6:201–214.
3. Gunawardena S, Goldstein LS. Cargo-carrying motor vehicles on the neuronal highway: transport pathways and neurodegenerative disease. J Neurobiol 2004;58:258–271.
4. Adio S, Reth J, Bathe F, Woehlke G. Regulation mechanisms of Kinesin-1. J Muscle Res Cell Motil 2006;27:153–160.
5. Gindhart JG. Towards an understanding of kinesin-1 dependent transport pathways through the study of protein-protein interactions. Brief Funct Genomic Proteomic 2006;5:74–86.
6. Gyoeva FK, Bybikova EM, Minin AA. An isoform of kinesin light chain specific for the Golgi complex. J Cell Sci 2000;113:2047–2054.
7. Wozniak MJ, Allan VJ. Cargo selection by specific kinesin light chain 1 isoforms. EMBO J 2006;25:5457–5468.
8. D'Andrea LD, Regan L. TPR proteins: the versatile helix. Trends Biochem Sci 2003;28:655–662.
9. Main ER, Xiong Y, Cocco MJ, D'Andrea L, Regan L. Design of stable alpha-helical arrays from an idealized TPR motif. Structure 2003;11:497–508.
10. Cliff MJ, Harris R, Barford D, Ladbury JE, Williams MA. Conformational diversity in the TPR domain-mediated interaction of protein phosphatase 5 with Hsp90. Structure 2006;14:415–426.
11. Gatto GJ Jr, Geisbrecht BV, Gould SJ, Berg JM. Peroxisomal targeting signal-1 recognition by the TPR domains of human PEX5. Nat Struct Biol 2000;7:1091–1095.
12. Scheufler C, Brinker A, Bourenkov G, Pegoraro S, Moroder L, Bartunik H, Hartl FU, Moarefi I. Structure of TPR domain-peptide complexes: critical elements in the assembly of the Hsp70-Hsp90 multichaperone machine. Cell 2000;101:199–210.
13. Lapouge K, Smith JS, Walker AP, Gamblin JS, Smerdon JS, Rittinger K. Structure of the TPR domain of p67phox in complex with Rac.GTP. Mol Cell 2000;6:899–907.
14. Coates JC. Armadillo repeat proteins: beyond the animal kingdom. Trends Cell Biol 2003;13:463–471.
15. Kobe B, Kajava AV. The leucine-rich repeat as a protein recognition motif. Curr Opin Struct Biol 2001;11:725–732.
16. Li J, Mahajan A, Tsai MD. Ankyrin repeat: a unique motif mediating protein-protein interactions. Biochemistry 2006;45:15168–15178.
17. Yaffe MB. How do 14-3-3 proteins work? – gatekeeper phosphorylation and the molecular anvil hypothesis. FEBS Lett 2002;513:53–57.
18. Bowman AB, Kamal A, Ritchings BW, Philp AV, McGrail M, Gindhart JG, Goldstein LS. Kinesin-dependent axonal transport is mediated by the sunday driver (SYD) protein. Cell 2000;103:583–594.
19. Byrd DT, Kawasaki M, Walcoff M, Hisamoto N, Matsumoto K, Jin Y. UNC-16, a JNK-signaling scaffold protein, regulates vesicle transport in C. elegans. Neuron 2001;32:787–800.
20. Verhey KJ, Meyer D, Deehan R, Blenis J, Schnapp BJ, Rapoport TA, Margolis B. Cargo of kinesin identified as JIP scaffolding proteins and associated signaling molecules. J Cell Biol 2001;152:959–970.
21. Whitmarsh AJ. The JIP family of MAPK scaffold proteins. Biochem Soc Trans 2006;34:828–832.
22. Kelkar N, Standen CL, Davis RJ. Role of the JIP4 scaffold protein in the regulation of mitogen-activated protein kinase signaling pathways. Mol Cell Biol 2005;25:2733–2743.
23. Nguyen Q, Lee CM, Le A, Reddy EP. JLP associates with kinesin light chain 1 through a novel leucine zipper-like domain. J Biol Chem 2005;280:30185–30191.
24. Horiuchi D, Barkus RV, Pilling AD, Gassman A, Saxton WM. APLIP1, a kinesin binding JIP-1/JNK scaffold protein, influences the axonal

transport of both vesicles and mitochondria in Drosophila. Curr Biol 2005;15:2137–2141.
25. Hurd DD, Saxton WM. Kinesin mutations cause motor neuron disease phenotypes by disrupting fast axonal transport in Drosophila. Genetics 1996;144:1075–1085.
26. Araki Y, Kawano T, Taru H, Saito Y, Wada S, Miyamoto K, Kobayashi H, Ishikawa HO, Ohsugi Y, Yamamoto T, Matsuno K, Kinjo M, Suzuki T. The novel cargo Alcadein induces vesicle association of kinesin-1 motor components and activates axonal transport. EMBO J 2007;26:1475–1486.
27. Bracale A, Cesca F, Neubrand VE, Newsome TP, Way M, Schiavo G. Kidins220/ARMS is transported by a kinesin-1-based mechanism likely to be involved in neuronal differentiation. Mol Biol Cell 2007;18:142–152.
28. McGuire JR, Rong J, Li SH, Li XJ. Interaction of Huntingtin-associated protein-1 with kinesin light chain: implications in intracellular trafficking in neurons. J Biol Chem 2006;281:3552–3559.
29. Ichimura T, Wakamiya-Tsuruta A, Itagaki C, Taoka M, Hayano T, Natsume T, Isobe T. Phosphorylation-dependent interaction of kinesin light chain 2 and the 14-3-3 protein. Biochemistry 2002;41:5566–5572.
30. Kamal A, Stokin GB, Yang Z, Xia CH, Goldstein LS. Axonal transport of amyloid precursor protein is mediated by direct binding to the kinesin light chain subunit of kinesin-I. Neuron 2000;28:449–459.
31. Kamm C, Boston H, Hewett J, Wilbur J, Corey DP, Hanson PI, Ramesh V, Breakefield XO. The early onset dystonia protein torsinA interacts with kinesin light chain 1. J Biol Chem 2004;279:19882–19892.
32. Kimura T, Watanabe H, Iwamatsu A, Kaibuchi K. Tubulin and CRMP-2 complex is transported via Kinesin-1. J Neurochem 2005;93:1371–1382.
33. Konecna A, Frischknecht R, Kinter J, Ludwig A, Steuble M, Meskenaite V, Indermuhle M, Engel M, Cen C, Mateos JM, Streit P, Sonderegger P. Calsyntenin-1 docks vesicular cargo to kinesin-1. Mol Biol Cell 2006; 17:3651–3663.
34. Ward BM, Moss B. Vaccinia virus A36R membrane protein provides a direct link between intracellular enveloped virions and the microtubule motor kinesin. J Virol 2004;78:2486–2493.
35. Reed NA, Cai D, Blasius TL, Jih GT, Meyhofer E, Gaertig J, Verhey KJ. Microtubule acetylation promotes kinesin-1 binding and transport. Curr Biol 2006;16:2166–2172.
36. Chen X, Kojima S, Borisy GG, Green KJ. p120 catenin associates with kinesin and facilitates the transport of cadherin-catenin complexes to intercellular junctions. J Cell Biol 2003;163:547–557.
37. Jinek M, Rehwinkel J, Lazarus BD, Izaurralde E, Hanover JA, Conti E. The superhelical TPR-repeat domain of O-linked GlcNAc transferase exhibits structural similarities to importin alpha. Nat Struct Mol Biol 2004;11:1001–1007.
38. Cai D, Hoppe AD, Swanson JA, Verhey KJ. Kinesin-1 structural organization and conformational changes revealed by FRET stoichiometry in live cells. J Cell Biol 2007;176:51–63.
39. Kelkar N, Gupta S, Dickens M, Davis RJ. Interaction of a mitogen-activated protein kinase signaling module with the neuronal protein JIP3. Mol Cell Biol 2000;20:1030–1043.
40. Sato S, Ito M, Ito T, Yoshioka K. Scaffold protein JSAP1 is transported to growth cones of neurites independent of JNK signaling pathways in PC12h cells. Gene 2004;329:51–60.
41. Kristensen O, Guenat S, Dar I, Allaman-Pillet N, Abderrahmani A, Ferdaoussi M, Roduit R, Maurer F, Beckmann JS, Kastrup JS, Gajhede M, Bonny C. A unique set of SH3-SH3 interactions controls IB1 homodimerization. EMBO J 2006;25:785–797.
42. Yasuda J, Whitmarsh AJ, Cavanagh J, Sharma M, Davis RJ. The JIP group of mitogen-activated protein kinase scaffold proteins. Mol Cell Biol 1999;19:7245–7254.
43. Bayarsaikhan M, Takino T, Gantulga D, Sato H, Ito T, Yoshioka K. Regulation of N-cadherin-based cell-cell interaction by JSAP1 scaffold in PC12h cells. Biochem Biophys Res Commun 2007;353: 357–362.
44. Muresan Z, Muresan V. c-Jun NH2-terminal kinase-interacting protein-3 facilitates phosphorylation and controls localization of amyloid-beta precursor protein. J Neurosci 2005;25:3741–3751.
45. Liu J, Taylor DW, Krementsova EB, Trybus KM, Taylor KA. Three-dimensional structure of the myosin V inhibited state by cryoelectron tomography. Nature 2006;442:208–211.
46. Thirumurugan K, Sakamoto T, Hammer JA III, Sellers JR, Knight PJ. The cargo-binding domain regulates structure and activity of myosin 5. Nature 2006;442:212–215.
47. Warren RA, Green FA, Stenberg PE, Enns CA. Distinct saturable pathways for the endocytosis of different tyrosine motifs. J Biol Chem 1998;273:17056–17063.
48. Haucke V. Cargo takes control of endocytosis. Cell 2006;127:35–37.
49. King SJ, Bonilla M, Rodgers ME, Schroer TA. Subunit organization in cytoplasmic dynein subcomplexes. Protein Sci 2002;11:1239–1250.
50. Tynan SH, Purohit A, Doxsey SJ, Vallee RB. Light intermediate chain 1 defines a functional subfraction of cytoplasmic dynein which binds to pericentrin. J Biol Chem 2000;275:32763–32768.
51. Tai AW, Chuang JZ, Sung CH. Cytoplasmic dynein regulation by subunit heterogeneity and its role in apical transport. J Cell Biol 2001;153: 1499–1509.
52. Mok Y-K, Lo KW, Zhang M. Structure of Tctex-1 and Its Interaction with cytoplasmic dynein intermediate chain. J Biol Chem 2001;276:14067–14074.
53. King SM, Barbarese E, Dillman JF, Benashski SE, Do KT, Patel-King RS, Pfister KK. Cytoplasmic dynein contains a family of differentially expressed light chains. Biochemistry 1998;37:15033–15041.
54. Waetzig V, Zhao Y, Herdegen T. The bright side of JNKs-multitalented mediators in neuronal sprouting, brain development and nerve fiber regeneration. Prog Neurobiol 2006;80:84–97.
55. Muresan Z, Muresan V. Coordinated transport of phosphorylated amyloid-beta precursor protein and c-Jun NH2-terminal kinase-interacting protein-1. J Cell Biol 2005;171:615–625.
56. Ha HY, Cho IH, Lee KW, Lee KW, Song JY, Kim KS, Yu YM, Lee JK, Song JS, Yang SD, Shin HS, Han PL. The axon guidance defect of the telencephalic commissures of the JSAP1-deficient brain was partially rescued by the transgenic expression of JIP1. Dev Biol 2005; 277:184–199.
57. Song JJ, Lee YJ. Cross-talk between JIP3 and JIP1 during glucose deprivation: SEK1-JNK2 and Akt1 act as mediators. J Biol Chem 2005; 280:26845–26855.
58. Kukekov NV, Xu Z, Greene LA. Direct interaction of the molecular scaffolds POSH and JIP is required for apoptotic activation of JNKs. J Biol Chem 2006;281:15517–15524.
59. Verhey KJ, Rapoport TA. Kinesin carries the signal. Trends Biochem Sci 2001;26:545–550.
60. Magliery TJ, Regan L. Beyond consensus: statistical free energies reveal hidden interactions in the design of a TPR motif. J Mol Biol 2004;343: 731–745.
61. Verhey KJ, Lizotte DL, Abramson T, Barenboim L, Schnapp BJ, Rapoport TA. Light chain-dependent regulation of Kinesin's interaction with microtubules. J Cell Biol 1998;143:1053–1066.
62. Whitmarsh AJ, Davis RJ. Structural organization of MAP-kinase signaling modules by scaffold proteins in yeast and mammals. Trends Biochem Sci 1998;23:481–485.
63. Meyer D, Liu A, Margolis B. Interaction of c-Jun amino-terminal kinase interacting protein-1 with p190 rhoGEF and its localization in differentiated neurons. J Biol Chem 1999;274:35113–35118.
64. Cavalli V, Kujala P, Klumperman J, Goldstein LS. Sunday driver links axonal transport to damage signaling. J Cell Biol 2005;168: 775–787.

65. Jones TA, Zou JY, Cowan SW, Kjeldgaard M. Improved methods for building protein models in electron density maps and the location of errors in these models. Acta Crystallogr A 1991;47:110–119.
66. Moore DD. Gene synthesis. In: Ausubel FM, Brent R, Kingston RE, Moore DD, Seidman JG, Smith JA, Struhl K, editors. Current Protocols in Molecular Biology. John Wiley and Sons, Inc. Hoboken, NJ; 2002, pp. 8.2.8–8.2.13.
67. Fromant M, Blanquet S, Plateau P. Direct random mutagenesis of gene-sized DNA fragments using polymerase chain reaction. Anal Biochem 1995;224:347–353.
68. Wilson DS, Keefe AD. Random mutagenesis by PCR. In: Ausubel FM, Brent R, Kingston RE, Moore DD, Seidman JG, Smith JA, Struhl K, editors. Current Protocols in Molecular Biology. John Wiley and Sons, Inc. Hoboken, NJ; 2002, pp. 8.3.1–8.3.4.
69. Yu JY, DeRuiter SL, Turner DL. RNA interference by expression of short-interfering RNAs and hairpin RNAs in mammalian cells. Proc Natl Acad Sci U S A 2002;99:6047–6052.
70. Matsuguchi T, Masuda A, Sugimoto K, Nagai Y, Yoshikai Y. JNK-interacting protein 3 associates with Toll-like receptor 4 and is involved in LPS-mediated JNK activation. EMBO J 2003;22:4455–4464.